

## Enhanced photoluminescence of hexamolybdenum cluster by anodic aluminum oxide photonic crystals

Thi Kim Ngan Nguyen<sup>a,\*</sup>, Hiroyo Segawa<sup>b</sup>, Fabien Grasset<sup>c,d</sup>, Stéphane Cordier<sup>c</sup>, Noée Dumait<sup>c</sup>, and Tetsuo Uchikoshi<sup>b,d,\*</sup>

<sup>a</sup>International Center for Young Scientists, National Institute for Materials Science, Ibaraki 305-0044, Japan

<sup>b</sup>Research Center for Electronic and Optical Materials, National Institute for Materials Science, Ibaraki 305-0044, Japan

<sup>c</sup>Univ. Rennes, CNRS, Institut des Sciences Chimiques de Rennes (ISCR)-UMR6226, F-35000 Rennes, France

<sup>d</sup>CNRS–Saint-Gobain–NIMS, IRL3629, Laboratory for Innovative Key Materials and Structures, National Institute for Materials Science, 1-1 Namiki, Ibaraki 305-0044, Japan

\*corresponding authors

### Abstract

The enhanced photoluminescence (PL) property of the Mo<sub>6</sub> cluster was first reported by its incorporation into an anodic aluminum oxide (AAO) matrix, a photonic structure to delocalize the emission light. Two kinds of AAO structures with different pore sizes, densities, and shapes were controlled by widening treatment for 3, 5, 7, and 10 minutes in phosphoric acid. Ordered AAO is able to narrow the PL peak at 680 nm while disordered AAO could shift the PL peak position in the NIR emission range with a high intensity obtaining more than 300% in comparison with that of MC deposited in ITO-glass. This result is interesting to apply for charged cluster-based materials in order to enhance luminescent quantum yields for photodetectors or biological applications.

**Keywords:** hexamolybdenum, octahedral cluster, anodic aluminum oxide, photoluminescence, electrochemistry.

### 1/ Introduction

In accordance with the increase in demand for optoelectronic devices, many studies on 1

1  
2  
3 nm-sized face-capped  $\{\text{Mo}_6\text{X}\}_8^i$  metallic cluster core ( $\text{X}^i = \text{I}, \text{Br}, \text{Cl}$ ) coordinated with  
4 apical ligands ( $\text{L}^a = \text{halogen}, \text{H}_2\text{O}, \text{OH}, \text{etc.}$ ) has been reported with high luminescent  
5 quantum yields for light-emitting diodes (LEDs), [1], biological applications [2] or visible  
6 light absorption for photodetectors [3], solar cells [4], and photocatalysts [5]. Only one  
7 study has revealed an enhancement of the photoluminescent (PL) properties of these  
8 metal clusters (MC) by using the engineering of 3D silica colloidal photonic crystals [6].  
9 In contrast, 3D inverse opal photonic crystal will enhance visible light absorption at the  
10 edge of stopband, resulting in an increase of photoinduced- electronic conduction  
11 properties of MC [3]. In connection with previous works, 1D anodic aluminum oxide  
12 (AAO) was investigated in narrowing or shifting the luminescent peak position and  
13 raising the luminescent intensity of MC. In addition to its great potential as a template for  
14 synthesizing 1D nanostructure, bandpass filter, or sensors, AAO photonic crystals have  
15 been approached to tune the structure color properties with other components [7-10].  
16 Similarly, 1D AAO photonic crystal film can create a photonic stopband that is controlled  
17 by periodic porosities and refractive index contrast. This dielectric periodic structure can  
18 generate a passband in the stopband that is tunable with PL emission light resulting in an  
19 intensity increase [11]. In this study, two kinds of AAO structures were prepared by  
20 electrochemistry in different electrolytes varying porosities and periodic structures. The  
21 negatively charged MC was deposited on the top or bottom of AAO by using  
22 electrophoretic deposition (EPD). The dependence of the PL peak position and PL  
23 intensity of MC on pore-widening treatment time which controls the refractive index as  
24 same as the stopband has been investigated. PL emission intensity around 680 nm of MC  
25 deposited on both AAOs was improved by more than 300%, moreover, the ordered AAO  
26 structure can narrow PL peak.  
27  
28  
29  
30  
31  
32  
33  
34  
35  
36  
37  
38  
39  
40  
41  
42  
43  
44  
45  
46

## 47 2/ Experimental

48 The AAO films were prepared by using alternating current oxidation, including four  
49 steps: polishing, anodizing, etching, and anodizing processes [9-10]. Detailed fabrications  
50 of disordered anodic aluminum oxide (DAAO) and ordered anodic aluminum oxide  
51 (OAAO) structures are illustrated in Table 1. The anodization was controlled to obtain a  
52 thickness of about 1  $\mu\text{m}$  in two structures. The pore-widening treatments for both  
53  
54  
55  
56  
57  
58  
59  
60  
61  
62  
63  
64  
65

structures were performed in 5%wt phosphoric acid for 3, 5, 7, and 10 minutes at ambient conditions. Pure aluminum plate (99,99%, 100×10×1 mm<sup>3</sup>) and the chemicals used without purification were purchased from the Wako Pure Chemistry Industry.

Table 1. Detailed fabrications of AAO films.

Structure	Polishing step	Anodizing step	Etching step	Anodizing step
<b>DAAO</b>	ethanol:	0.02v%	6wt%	0.02v% phosphoric
	perchloric (4:1/v:v); 2 mA;	2 150V; 3 hours; 12°C	phosphoric acid and 1.8wt%	acid; 150 V; 25 minutes and 6 mA; 1 hour
<b>OAAO</b>	minutes; 10°C	0.15 M oxalic acid; 3 hours; 40 V; 20°C	chromic acid; 3 hours; 60°C	0.15 M oxalic acid; 40 V; 8 minutes and 6 mA; 1 hour; 20°C

Cs<sub>2</sub>[{Mo<sub>6</sub>Br<sup>i</sup><sub>8</sub>}Br<sup>a</sup><sub>6</sub>] compound (MC) was synthesized following the reported procedure [12]. CMB was disassociated in methyl ethyl ketone (MEK, 99 %) at a concentration of 2.5 g/l. EPD of MC on ITO-coated glass and AAO substrates was optimized at 12 V for 60 seconds [13]. EPD was built of stainless-steel cathode and ITO glass (Geomatec Co., 7 Ohm/sq) or AAO anodes that were connected to an electric field generator (Keithley Model 2400, SA). MC deposited on AAO films was characterized by FE-SEM, reflectance, and photoluminescence (PL).

### 3/ Results and discussion

DAAO structure was successfully prepared as seen in Figs. 1a-b. DAAO reflects mixed colors due to the strong interference of reflecting light from a periodic structure. The irregularly shaped porosities show various diameters lower than 300 nm, accompanied by a stem layer length of 600 nm and a branched layer length of 200 nm. The negative charge on the [{Mo<sub>6</sub>Br<sup>i</sup><sub>8</sub>}Br<sup>a</sup><sub>6</sub>]<sup>2-</sup> cluster brings an essential advantage to introduce inside the pore of DAAO by using EPD with reported MC formula as [{Mo<sub>6</sub>Br<sup>i</sup><sub>8</sub>}Br<sup>a</sup><sub>4</sub> (H<sub>2</sub>O)<sup>a</sup><sub>2</sub>] [13]. The deposition of MC on the surface and stem porosities of OAAO before and after widening for 3 minutes is an insignificant difference, observed with big MC particles as signed in yellow circles (Figs. 1c-d). From SEM-EDX mapping and spectra, the Mo element is confirmed mostly at the surface of DAAO (Figs. 1e-f).

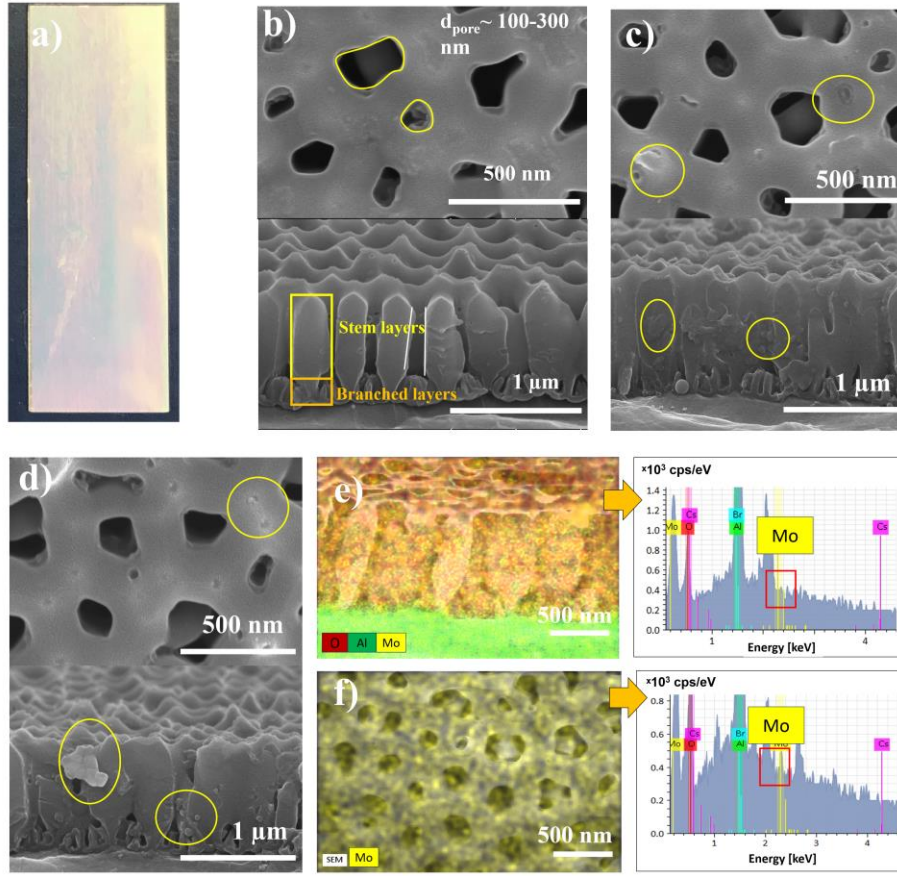
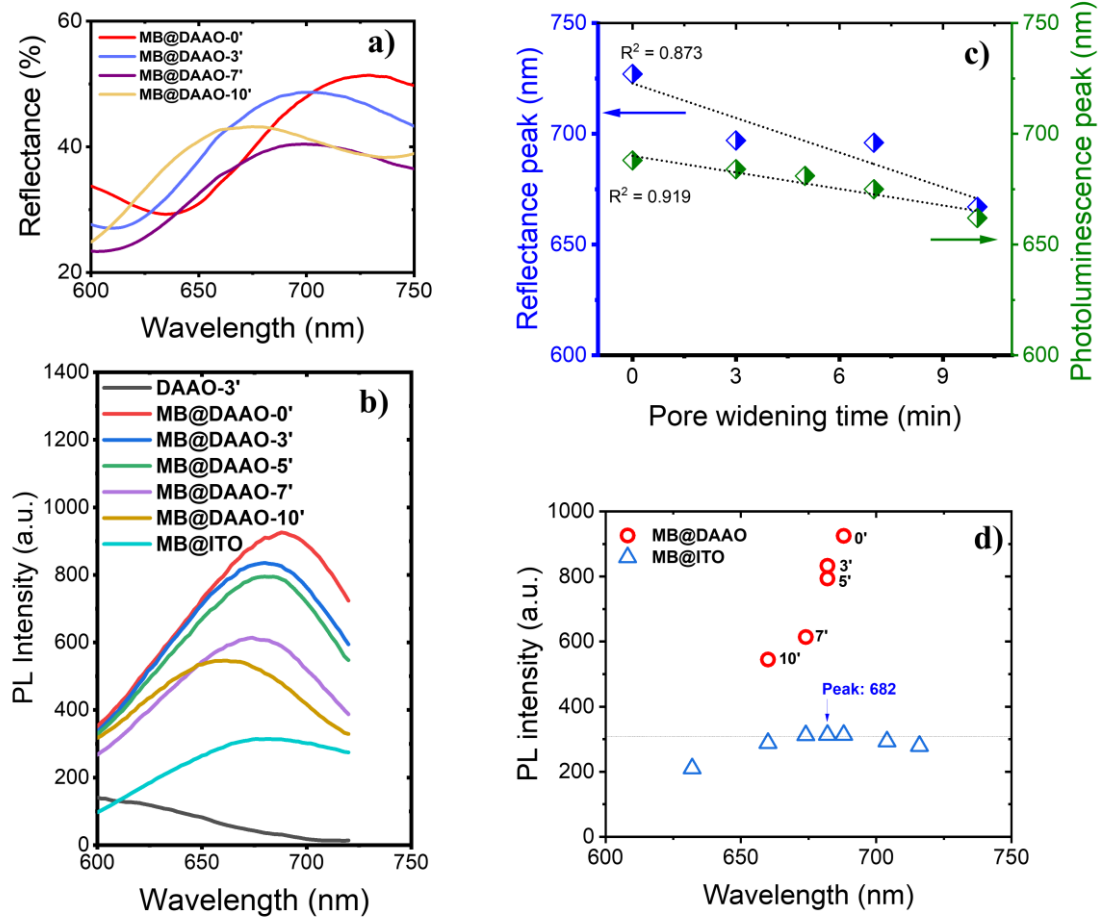


Figure 1. a) Photograph of DAAO. FE-SEM images of the surface and cross-section of b) DAAO, c) MC@DAAO, and d) MC@DAAO widened for 3 minutes. SEM-EDX mapping images of e) cross-section and f) surface of MC@DAAO widened for 3 minutes.

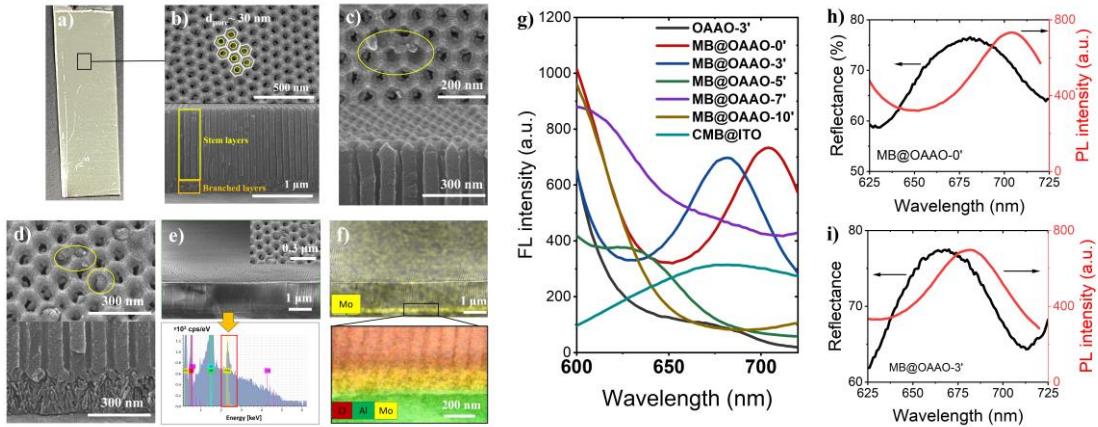
The optical properties of MC deposited on DAAO films with pore-widening treatment for 0, 3, 5, 7, and 10 minutes are demonstrated in Figs. 2a-b. The treatment causes the different periodic structures and provides the distinctive interfering of reflectance (Fig. 2a). DAAO films show reflectance peaks in the range from 668 and 727 nm that are close to PL peak of MC at 680 nm (Fig. 2b). The tunable optical effect between MC and DAAO was investigated. An essential factor that will contribute to enhanced PL intensity is the position of the reflectance peak of DAAO. The approximate stopband position of AAO can be calculated by Bragg's law that is expressed in Eq. 1 while ignoring the effect of branched layers [7]:

$$\lambda_{\max} = 2l_{\text{stem}} \sqrt{n_{\text{stem}}^2 - \sin^2\theta} \quad (1)$$

Where  $\lambda$  is the stopband position for the first-order Bragg diffraction,  $n_{\text{stem}}$  is the refractive indices of AAO ( $\sim 1.685$ ), and  $\theta$  is the incidence angle of the light ( $5^\circ$ ). In general, pore-widening treatment mainly increases the porosities of stem layers that contain air ( $n_{\text{air}} \sim 1$ ), resulting in a decrease in the effective refractive index. Following Eq. 1, reflectance peaks will shift to a lower wavelength. As a consequence, PL peaks obtain a similar decreasing trend. The linear dependence of the reflectance and PL peaks on the pore-widening time is similar and confirmed with different rates in Fig. 2c. This result indicates the independence of treatment or PL and reflectance peaks on stem layer length. The PL intensity of MC significantly increases in corporation with DAAO for all widening times. A treatment time lower than 5 minutes is efficient for controlling the reflectance peak around the PL peak of MC, increasing PL intensity by more than 300% (Fig. 2d). Summarily, the intensity and position of the PL peak are modified in the range limited by broad PL spectrum of MC as deposited on ITO glass.



1  
2  
3 Figure 2. a) Reflectance spectra and b) PL spectra of MC@DAAO widened at different  
4 times and excitation wavelength of 365 nm. C) Dependence of reflectance and PL peak  
5 of MC@DAAO on widening time. D) PL intensity of MC@ITO and MC@DAAO.  
6  
7  
8 The FE-SEM images of OAAO confirm uniform circle pores with a diameter of  $29 \pm 5$  nm,  
9 and stem layer length of 1100 nm (Figs 3a-b). Oxalic acid is more efficient than  
10 phosphoric acid to form an ordered AAO structure. MC deposition is confirmed on the  
11 surface of OAAO films without and with treatment (Figs. 3c-d). SEM-EDX mapping and  
12 element spectra indicated the Mo elements concentrate on branched layers (Figs. 3e-f).  
13 Similarly, OAAO also provides the tunable light emission at around 680 nm which is the  
14 PL peak of MC, increasing intensity by more than 200% (Fig. 3g). In addition, the PL  
15 peak shape is narrowed in a shortening range between 650 and 750 nm while the range is  
16 580 nm and 800nm for MC deposited on flat ITO glass. From Figs. 3h-i, the synchronized  
17 shift of reflectance and PL peak position to a lower wavelength occurs when pore-  
18 widening treatment is performed. The differently narrowing effects of DAAO and OAAO  
19 on PL peaks also come from MC depositing positions, reflectance peak shape, etc. A deep  
20 study of the contribution of the interference phenomenon coming from the AAO structure  
21 on the PL peak of MC will be carried out.



34  
35  
36  
37  
38  
39  
40  
41  
42  
43  
44  
45  
46  
47  
48  
49  
50  
51  
52  
53  
54  
55  
56  
57  
58  
59  
60  
61  
62  
63  
64  
65  
Figure 3. a) Photograph of OAAO. FE-SEM images of the surface and cross-section of  
b) OAAO, c) MC@OAAO, and d) MC@OAAO widened for 3 minutes. e) element  
spectra and f) SEM-EDX mapping images of MC@OAAO surface widened for 3 minutes.  
G) PL spectra of MC@OAAO widened at different times. The correlation between  
reflectance and PL peak positions of MB@OAAO h) without and i) with widening for 3

1  
2  
3 minutes.

#### 4/ Conclusions

5  
6 The depositing position of MC in the bottom of OAAO efficiently narrows PL peak shape  
7 and pore-widening treatment in DAAO efficiently works in slow modification in PL peak  
8 position. Although MC amount on AAO films ( $\sim 0.058 \text{ mg/cm}^2$ ) is less than that on ITO  
9 glass ( $\sim 0.368 \text{ mg/cm}^2$ ), the PL intensity of MC which is tunable optical properties of both  
10 AAO structures was enhanced by about 200% or 300% in comparison with MC deposited  
11 on the flat ITO-glass. This study will provide a new concept for developing enhanced  
12 luminescent material based on metal clusters for energy-related applications and sensors.  
13  
14  
15  
16  
17  
18  
19  
20

#### Acknowledgment

21  
22 These studies were carried out under the continued financial support of the International  
23 Center for Young Scientists (NIMS) and the France-Japan International Collaboration  
24 Framework (IRL3629 LINK, ANR-22-CE09-0015).  
25  
26  
27  
28  
29

#### References

- 30  
31 [1] Kuttipillai, P. S., et al. Diodes., *Adv. Mater.*, 28 (2016) 320-326.  
32  
33 [2] K. Kirakci, M. A. Shestopalov, K. Lang. *Coordination Chemistry Reviews*, 481(2023),  
34 215048.  
35  
36 [3] T.K.N. Nguyen, F. Grasset, S. Cordier, N. Dumait, S. Ishii, H. Fudouzi, T. Uchikoshi,  
37 *Material Today Chemistry*, 27 (2023), 101351.  
38  
39 [4] A. Renaud, T.K.N. Nguyen, F. Grasset, M. Raissi, V. Guillon, F. Delabrouille, N.  
40 Dumait, P.-Y. Jouan, L. Cario, S. Jobic, Y. Pellegrin, F. Odobel, S. Cordier, T. Uchikoshi.  
41 *Electrochimica Acta*, 317 (2019) 737-745.  
42  
43 [5] M.P. Atienzar, M. Amela-Cortes, N. Dumait, P. Lemoine, Y. Molard, S. Cordier.  
44 *Inorg.Chem.* 58 (2019) 15443–15454.  
45  
46 [6] J.F. Dechézelles, T. Aubert, F. Grasset, S. Cordier, C. Barthou, C. Schwob, A. Maître,  
47 R. A L Vallée, H. Cramail, S. Ravaine. *Phys Chem Chem Phys*, 12 (2010)11993-11999.  
48  
49 [7] H. Wei, Q. Xu, D. Chen, M. Chen, M. Chang, X. Ye, *Optical Materials*, 122 (2021)  
50 111722.  
51  
52 [8] H. Wang, M. Li, Z. Yin, T. Zhang, X. Chen, D. Zhou, J. Zhu, W. Xu, H. Cui, H. Song.  
53  
54  
55  
56  
57  
58  
59  
60  
61  
62  
63  
64  
65

1  
2 ACS Appl. Mater. Interfaces, 9 (2017), 37128–37135.

3  
4 [9] K. Sekiguchi, K. Katsumata, H. Segawa, T. Nakanishi, and A. Yasumori. ACS Appl.  
5 Mater. Interfaces, 12 (2020) 27672–27681.

6  
7 [10] S.Z. Chu, K. Osaka, H. Yashiro, H. Segawa, K. Wada, and S. Inoue. ECS  
8 Transactions, 58 (38) 61-70 (2014)

9  
10 [11]C. I. Aguirre, E. Reguera, A. Stein. Adv. Funct.Mater., 20 (2015), 2565-2578.

11  
12 [12] 15.K. Kirakci, S. Cordier and C. Perrin, Z. Anorg. Allg. Chem., 631 (2005), 411-416.

13  
14 [13] 16.T. K. N. Nguyen, B. Dierre, F. Grasset, A. Renaud, S. Cordier, P. Lemoine, N.  
15 Ohashi and T. Uchikoshi, J. Electrochem. Soc., 164 (2017) D412.  
16  
17  
18  
19  
20  
21  
22  
23  
24  
25  
26  
27  
28  
29  
30  
31  
32  
33  
34  
35  
36  
37  
38  
39  
40  
41  
42  
43  
44  
45  
46  
47  
48  
49  
50  
51  
52  
53  
54  
55  
56  
57  
58  
59  
60  
61  
62  
63  
64  
65

**Declaration of interests**

The authors declare that they have no known competing financial interests or personal relationships that could have appeared to influence the work reported in this paper.

The authors declare the following financial interests/personal relationships which may be considered as potential competing interests:

We have no competing interests.